SYNCHRONY-BREAKING HOPF BIFURCATION IN A MODEL OF ANTIGENIC VARIATION

BERNARD S. CHAN* and PEI YU†
Department of Applied Mathematics,
The University of Western Ontario, London,
Ontario, Canada N6A 5B7
*bchan6@uwo.ca
†pyu@uwo.ca

In this paper, we will analyze the bifurcation dynamics of an *in vivo* model of *Plasmodium falciparum*. The main attention of this model is focused on the dynamics of cross-reactivity from antigenic variation. We apply the techniques of coupled cell systems to study this model. It is shown that synchrony-breaking Hopf bifurcation occurs from a nontrivial synchronous equilibrium. In proving the existence of a Hopf bifurcation, we also discover the condition under which possible 2-color synchrony patterns arise from the bifurcation. The dynamics resulting from the bifurcation are qualitatively similar to known behavior of antigenic variation. These results are discussed and illustrated with specific examples and numerical simulations.

Keywords: Hopf bifurcation; stability; antigenic variation; multiple strains; infectious disease.

1. Introduction

Antigenic variation is a successful strategy for pathogens to evade the immune system [Craig & Scherf, 2003]. The exact process is not well-understood yet. We first give a summary of the currently accepted view on the subject here. Precursor cells of the immune system detect potential pathogens via specific chemical determinants, such as proteins and carbohydrates, on the surfaces of pathogens or infected cells. These chemical markers are called epitopes. Once detected, precursor cells may differentiate into effector cells and eliminate the potential threat. In the continual battle between pathogens and the immune system, some pathogens have evolved to have a wide variety and seemingly ever changing surface markers. Antigen specific precursors may fail to recognize them as harmful material immediately. This delay in recognition allows

the pathogen population time to grow so that it can express another surface protein. By the time the effectors have cleared away one variant, another variant of the same pathogen would be growing. This strategy of presenting many different variants by the pathogens for the purpose of evading the immune system is called antigenic variation. Different variants can arise from point mutations of the pathogen, thus giving rise to new variants with different genotypes. Alternatively, it can arise from programmed variation of the surface markers. In this case, the different surface markers are simply the expression of the same genetic structures.

Plasmodium falciparum is a pathogen capable of antigenic variation and it causes malaria in humans. In this paper, we will analyze the bifurcation dynamics of an ordinary differential equation model of this protozoan parasite, originally

---

†Author for correspondence

proposed by Recker *et al.* [2004]. Research shows that the variants of *P. falciparum* presented inside the hosts are different phenotypes stemming from the *var* gene [Turner, 2002]. On the surface of these different variants are various epitopes. This model assumes that there are major epitopes that are unique to each variant and minor epitopes that are shared across variants. It has been hypothesized that the major epitope from each variant elicits longterm CTL response that is variant specific. On the other hand, the minor epitopes that are shared by multiple variants elicit transient CTL response that will cross-react to any strains which share the minor epitope. The dynamics resulting from this feature of antigenic variation was the focus in [Recker *et al.*, 2004] and will be further examined analytically in this work.

Given that the interactions between *P. falciparum* and the immune system are not well understood, there are mathematical models in the literature studying the dynamics. Single variant model of the in-host dynamics has been considered by Saul [1998] and Gravenor and Lloyd [1998]. Mutation dynamics of multistrain pathogens have been studied in [De Leenheer & Pilyugin, 2008b]. Furthermore, stochastic models of antigenic variation have been reviewed in [Frank & Barbour, 2006]. For deterministic models, Recker *et al.* [2004] proposed a differential equation model, which describes the effects of antigenic variations on immune effectors and pathogens. This aforementioned model allows one to connect different sets of differential equations to examine the effects of immune cross-protection incited from shared epitopes between variants. Specific cases from the aforementioned model have been further studied numerically and analytically in [Blyuss & Gupta, 2009]. Mitchell and Carr [2010, 2012] considered the effects of time delay in the production of cross-reactive immune cells for the model in [Recker *et al.*, 2004] in their works.

In this paper, we will add to the study of antigenic variation models by examining the bifurcation structure analytically for a general case described in [Blyuss & Gupta, 2009]. In Sec. 2, we will describe the model on antigenic variation described in [Blyuss & Gupta, 2009]. Next, we will show that the linear structure for this model can be studied using the techniques as described by Golubitsky and Lauterbach [2009] in Sec. 3. In Sec. 4, we use the simplified linear structure and techniques in [Yu,

2005] to analytically determine the Hopf bifurcation which occurs from the fully synchronous equilibrium. Numerical simulations showing the earlier analytic results are provided in Sec. 5. In Sec. 6, we discuss the biological implications based on insights gained from the mathematical analysis of the model.

2. The Model

In 2004, Recker *et al.* proposed their multivariant within-host antigenic variation model of malaria, which was further studied in [Blyuss & Gupta, 2009] and its characteristics are described here. It is assumed that each variant of the pathogen, represented by y_i, shares minor epitopes with other variants. Each major variant is unique and we assume that the major epitope belonging to the variant elicits a long-lived immune response z_i. Similarly, the minor epitopes also bring forth immune responses from the host, but the responses caused by the minor epitopes w_i are assumed to be transient and cross-reactive. A particular variant i and its interactions with the immune system are described by

$$
\begin{aligned}
\frac{dy_i}{dt} &= y_i(\phi - \alpha_1 z_i - \alpha_2 w_i), \\
\frac{dz_i}{dt} &= \beta_1 y_i - \mu_1 z_i, \\
\frac{dw_i}{dt} &= \beta_2 \left(y_i + \sum_{l \sim i} y_l \right) - \mu_2 w_i.
\end{aligned}
\tag{1}
$$

In this model, specific variant i of the pathogen is produced at the constant rate ϕ, and this pathogen population is eliminated by the long-lived and transient immune responses at rates α_1 and α_2, respectively. The host immune system produces the long-lived response at rate β_1 when it is stimulated by y_i and it has a natural decaying rate of μ_1. We use $l \sim i$ to denote the set of all variants that share a minor epitope with variant i. Given that the transient response is triggered by any variants of the pathogen that shares a particular minor epitope, the growth rate of the transient response is proportional to $y_i + \sum_{l \sim i} y_l$ at rate β_2 and it has a natural decaying rate of μ_2.

As shown in [Recker *et al.*, 2004], this model can be extended to study the effects of many major variants with numerous minor epitopes. The general case can be difficult to analyze with

analytic methods due to large number of variables. Potentially, there can be many different configurations based on biological conditions. Mathematically, these configurations correspond to different coupling structures consisting of system (1). In this paper, we will study the case proposed in [Blyuss & Gupta, 2009] when each variant can have two minor epitopes and there are finite number of minor epitope variants.

3. Antigenic Variation Model as a Product Network

To study the effects of cross-reactivity, one would describe the dynamics of each variants of *P. falciparum* with the set of differential equations in system (1) and couple these systems based on shared epitopes amongst variants. As stated in [Blyuss & Gupta, 2009], the simplest nontrivial case is when each variant of the pathogen has two different minor epitopes. Even with such few variants and couplings, it is still difficult to analyze the dynamics of the system analytically. In this section, we will show that when each variant of the *P. falciparum* has only two minor epitopes, the model can be described as the product network of two all-to-all networks as described in [Golubitsky & Lauterbach, 2009]. By recasting the model in a connected network, we can utilize the methods of coupled cell systems [Golubitsky *et al.*, 2005] to analyze stability and bifurcation of equilibria and their dynamics are studied in Sec. 4.

To carry out the analysis, we first describe the theory necessary. In the terminology employed by Golubitsky and Stewart [2006] and the references therein, a *cell*, or *node*, of the directed graph, represents a system of ordinary differential equations and a *coupled cell system* is a network of nodes coupled with each other. Couplings between the differential equation systems are graphically represented using a digraph. The shape, or label, of a node is used to indicate a particular system of differential equations. Let $\mathcal{C}$ denote the set of nodes and $\sim_{\mathcal{C}}$ denote an equivalence relation of nodes on $\mathcal{C}$. Similarly, the shape of the *arrow*, or a *directed edge*, indicates the type of coupling between two nodes. Let $\mathcal{E}$ denote the set of edges and $\sim_{\mathcal{E}}$ denote an equivalence relation of edges on $\mathcal{E}$. For each $e \in \mathcal{E}$, the functions $\mathcal{H} : \mathcal{E} \to \mathcal{C}$ and $\mathcal{T} : \mathcal{E} \to \mathcal{C}$ denote the node at the *head* and *tail* of e, respectively. Two arrows are equivalent if they have equivalent tails and heads

(i.e. for $e_1, e_2 \in \mathcal{E}, e_1 \sim_{\mathcal{E}} e_2 \Rightarrow \mathcal{H}(e_1) \sim_{\mathcal{C}} \mathcal{H}(e_2)$ and $\mathcal{T}(e_1) \sim_{\mathcal{C}} \mathcal{T}(e_2)$).

In general, the framework of coupled cell systems allows for different types of nodes and couplings mixed together in one system. A system that has only one type of node is called *homogenous* and similarly, a system with only one type of arrow is called *regular*. In other words, a regular homogenous n-node network is composed of identical systems of differential equations which are coupled together with identical coupling terms.

Using the method described in [Golubitsky & Lauterbach, 2009], any two coupled cell systems can be formed as a product network. Suppose that N_1 and N_2 are two regular homogenous coupled cell networks with node sets $\mathcal{C} = \{c_1, \ldots, c_{n_1}\}$ and $\mathcal{D} = \{d_1, \ldots, d_{n_2}\}$, respectively. We form a product network $N = N_1 \boxtimes N_2$ by replacing each node c_i in N_1 by a copy of N_2. Let p_{ij} represent the node in N that is from the jth node in the copy of N_2 which replaces the ith node in N_1. There is a coupling from node p_{ij} to p_{lj} if and only if there is a coupling from c_i to c_l in N_1. Furthermore, there is a coupling from p_{ij} to p_{il} if and only if there is a coupling from d_j to d_l. This convention for forming a product network allows for the nodes as well as the couplings from N_1 and N_2 to be distinct from each network.

Applying the aforementioned theory in the context of the antigenic variation models [Recker *et al.*, 2004; Blyuss & Gupta, 2009], each node represents the differential equations in system (1), which in turn describes the dynamics for a particular variant i of the pathogen. As mentioned earlier, when two major variants share a variant of the minor epitope, they are coupled with each other. Based on the third equation in system (1), the coupling between any variants must be the same. Since there is only one set of differential equations and one kind of couplings, any coupled cell network formed by coupling copies of system (1) together would be a regular homogenous coupled cell network. For the case when there are two minor epitopes, we suppose that there are n_1 classes with the first minor epitope and n_2 classes with the second minor epitope.

In the next theorem, we will show that the model of antigenic variation can be constructed through the product networks of two all-to-all connected networks. Given that the digraphs for the networks constructed using the following theorem lack the self-couplings on each node that are present

in the digraphs of the networks shown in [Blyuss & Gupta, 2009], we will show in Theorem 2 that the networks are ODE-equivalent as described in [Dias & Stewart, 2005].

Theorem 1. *Suppose there are two minor epitopes for each variant of the pathogen and there are n_1 and n_2 classes for each minor epitope, respectively. Let N_1 be an n_1-node all-to-all connected network and similarly let N_2 be an n_2-node all-to-all connected network. Let nodes in N_1 and N_2 be represented by system (1). Then, the product network $N = N_1 \boxtimes N_2$ satisfies the biological requirement as set out in [Blyuss & Gupta, 2009]. That is, each variant which shares a minor epitope must be coupled.*

Proof. We label the nodes of N_1 as $c_1, \ldots, c_{n_1}$ and those of N_2 as $d_1, \ldots, d_{n_2}$. To construct $N = N_1 \boxtimes N_2$, we replace the ith node in N_1 with a copy of N_2. There are $n_1 n_2$ nodes in N and we denote these new nodes as p_{ij}, with index i corresponding to the ith node in N_1 that has been replaced with N_2. The index j refers to the jth node in N_2 which replaces the ith node in N_1.

The rule in creating a product network dictates that there is a coupling from p_{ij} to p_{il} if and only if there is a coupling from d_j to d_l. This rule implies that all nodes with the same index i must have a coupling between them. Since nodes having the same index i must share the same variant of a minor epitope, this rule and the fact that N_2 is an all-to-all connected network ensure that all nodes sharing a variant of the minor epitope belonging to N_2 are coupled. With the rules regarding the second index, there is a coupling from node p_{ij} to p_{lj} if and only if there is a coupling from c_i to c_l in N_1. Again, this rule and the fact that N_1 is also an all-to-all connected network ensure that all nodes sharing the variant of minor epitope in N_1 must be coupled. Hence, we have shown that all nodes that share a variant minor epitope would share a coupling as described in [Blyuss & Gupta, 2009]. ∎

We provide an example of applying Theorem 1 in Fig. 1. Two 2-node all-to-all connected networks are combined to represent the dynamics with four variants and each having two minor epitopes. The same dynamics are described by a different example in [Blyuss & Gupta, 2009], but the digraph shown in that paper has self-couplings for each node that are not present in our work. While the representing
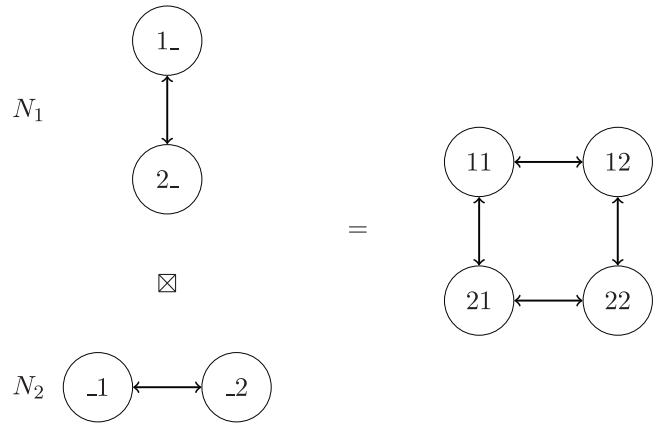

Fig. 1. An example of forming a new network with two other networks based on Theorem 1: N_1 and N_2 are both 2-node all-to-all connected networks; and the resulting network has four nodes in the network.

digraphs differ, we will show that these two representations are equivalent.

As mentioned by Golubitsky *et al.* [2005], two different digraphs representing coupled cell systems can have the same admissible vector fields and such networks are called *ODE-equivalent*. Let $\mathbf{x} \in \mathbb{R}^3$, then the admissible vector fields for the representation shown in [Blyuss & Gupta, 2009] have the form

$$H(\mathbf{x}_1, \mathbf{x}_2, \mathbf{x}_3, \mathbf{x}_4)$$
$$= (h(\mathbf{x}_1, \mathbf{x}_1, \mathbf{x}_2, \mathbf{x}_4), h(\mathbf{x}_2, \mathbf{x}_2, \mathbf{x}_1, \mathbf{x}_2),$$
$$h(\mathbf{x}_3, \mathbf{x}_3, \mathbf{x}_2, \mathbf{x}_4), h(\mathbf{x}_4, \mathbf{x}_4, \mathbf{x}_3, \mathbf{x}_1)),$$

where $h : (\mathbb{R}^3)^4 \to \mathbb{R}^3$ is a smooth function. For the system shown in Fig. 1, the admissible vector fields take the form

$$F(\mathbf{x}_1, \mathbf{x}_2, \mathbf{x}_3, \mathbf{x}_4) = (f(\mathbf{x}_1, \mathbf{x}_2, \mathbf{x}_4), f(\mathbf{x}_2, \mathbf{x}_1, \mathbf{x}_2),$$
$$f(\mathbf{x}_3, \mathbf{x}_2, \mathbf{x}_4), f(\mathbf{x}_4, \mathbf{x}_3, \mathbf{x}_1)),$$

where $f : (\mathbb{R}^3)^4 \to \mathbb{R}^3$ is a smooth function. One can see that the set $\{H\}$ of all H is the same as the set of $\{F\}$ of all F. For any given f, we can set $h(\mathbf{x}_i, \mathbf{x}_i, \mathbf{x}_j, \mathbf{x}_k) = f(\mathbf{x}_i, \mathbf{x}_j, \mathbf{x}_k)$, so clearly $\{H\} \subseteq \{F\}$. Conversely, for any given h we can set $f(\mathbf{x}_i, \mathbf{x}_j, \mathbf{x}_k) = h(\mathbf{x}_i, \mathbf{x}_i, \mathbf{x}_j, \mathbf{x}_k)$, so that $\{F\} \subseteq \{H\}$. Hence, we have shown that $\{F\} = \{H\}$ and thus shown that the two formulations of the networks are ODE-equivalent in the sense of Dias and Stewart [2005]. In general, we can summarize the equivalence between the systems formed in Theorem 1 and the networks formed in [Blyuss & Gupta, 2009] in the next theorem.

Theorem 2. *Suppose N_1 and N_2 are all-to-all connected networks and each has n_1 and n_2 nodes, respectively. Then, any network $N = N_1 \boxtimes N_2$ formed using Theorem 1 describes the same $S_{n_1} \times S_{n_2}$ model of antigenic variation as described in [Blyuss & Gupta, 2009].*

Proof. A direct comparison of the digraph representing N and the one representing that in $S_{n_1} \times S_{n_2}$ system will show that they only differ by the lack of self-couplings in the digraph representing N. We can repeat our earlier argument for ODE-equivalence between the examples in Fig. 1 and the same as the example shown in [Blyuss & Gupta, 2009] for networks of any size. With ODE-equivalence and each node in the networks representing the same system (1), the system trivially describes the same model of antigenic variation as needed. ∎

In studying this antigenic variation model, N_1 and N_2 have the same type of nodes and coupling structures, so $N_1 \boxtimes N_2$ is the same as $N_2 \boxtimes N_1$. For the sake of clarity and convenience, we introduce new index notations for systems formed under Theorem 1. Suppose $N = N_1 \boxtimes N_2$, then we form the system as

$$\frac{dy_{ij}}{dt} = y_{ij}(\phi - \alpha_1 z_{ij} - \alpha_2 w_{ij}),$$

$$\frac{dz_{ij}}{dt} = \beta_1 y_{ij} - \mu_1 z_{ij},$$

$$\frac{dw_{ij}}{dt} = \beta_2 \left(y_{ij} + \sum_{l \in I_i}^{n} y_{lj} + \sum_{l \in J_j}^{m} y_{il} \right) - \mu_2 w_{ij}, \quad (2)$$

where $i \in \{1, \dots, n_1\}$ and $j \in \{1, \dots, n_2\}$. Let $\mathbf{x}_{ij} = (y_{ij}, z_{ij}, w_{ij})^T$ and let I_i and J_j represent index sets consisting of the indices which are connected to node ij via the first and the second positions, respectively. We define the function $F : \mathbb{R}^3 \to \mathbb{R}^3$ such that the vector differential equation

$$\frac{d\mathbf{x}_{ij}}{dt} = \mathbf{F}(\mathbf{x}_{ij}, \mathbf{x}_{I_i,j}, \mathbf{x}_{i,J_j}) \quad (3)$$

represents the general network formed in Theorem 1.

4. Stability and Bifurcation Analysis

The system formed based on Theorem 1 has $2^{n_1 n_2}$ equilibria [Blyuss & Gupta, 2009]. Of all these equilibria, there are two fully synchronous equilibria, given by

$$\mathbf{x}_1^* = (y_1^*, z_1^*, w_1^*)^T = (0, 0, 0)^T, \quad \text{and}$$

$$\mathbf{x}_2^* = (y_2^*, z_2^*, w_2^*)^T$$

$$= \left(\frac{\phi \mu_1 \mu_2}{\alpha_1 \beta_1 \mu_2 + n_c \alpha_2 \beta_2}, \frac{\beta_1 \phi \mu_2}{\alpha_1 \beta_1 \mu_2 + n_c \alpha_2 \beta_2}, \right.$$

$$\left. \frac{\beta_2 \phi \mu_1}{\alpha_1 \beta_1 \mu_2 + n_c \alpha_2 \beta_2} \right)^T,$$

where $\mathbf{x}_i^*$ represents the equilibrium expression for each node and $n_c = n_1 + n_2 - 2$ denotes the number of connections per node. Clearly, $\mathbf{x}_1^*$ corresponds to trivial dynamics for a biological model. We will investigate the stability at these equilibria as well as possible bifurcations from these equilibria. Stability of the synchronous equilibria will be analyzed using the product network structure and bifurcations will be analyzed based on balanced coloring and quotient networks.

4.1. *Local stability near* $\mathbf{x}_1^*$

To understand the stability of the two synchronous equilibria, we describe the Jacobian structure of a system formed using product networks. Suppose N_1 and N_2 are two coupled cell systems with A_1 and A_2 as the respective adjacency matrix. Based on the adjacency matrices, linearized internal and coupling dynamics, we can directly find the expression of the Jacobian at any fully synchronous equilibria [Golubitsky & Lauterbach, 2009]. If N_1 has n_1 nodes and N_2 has n_2 nodes, then the Jacobian matrix for $N = N_1 \boxtimes N_2$ can be written as

$$J = \eta \otimes \mathbf{I}_{r_1} \otimes \mathbf{I}_{r_2} + \gamma_1 \otimes A_1 \otimes \mathbf{I}_{r_2} + \gamma_2 \otimes \mathbf{I}_{r_1} \otimes A_2,$$

where $\otimes$ denotes tensor products between two matrices, $\eta \in \mathbb{R}^{k \times k}$ is linearized internal dynamics of N_2 and $\gamma_1, \gamma_2 \in \mathbb{R}^{k \times k}$ are the linearized coupling dynamics in networks N_1 and N_2, respectively. Furthermore, the eigenvalues of J are the same as the eigenvalues of

$$M_{u,v} = \eta + u\gamma_1 + v\gamma_2, \quad (4)$$

where $u \in \text{spec}(A_1)$ and $v \in \text{spec}(A_2)$. In other words, one knows the entire eigenvalue structure of a product network system by only knowing the linearized internal dynamics, linearized coupling dynamics, and the eigenvalues of the adjacency matrices of N_1 and N_2.

In application to antigenic variation model, we shall now find the linearized internal dynamics, linearized coupling dynamics, and the eigenvalues of the adjacency matrices of N_1 and N_2. Through a direct calculation, the linearized internal dynamics of each node is

$$\eta = (d\mathbf{F})_{\mathbf{x}_{ij}} = \begin{pmatrix} \phi - \alpha_1 z - \alpha_2 w & -\alpha_1 y & -\alpha_2 y \\ \beta_1 & -\mu_1 & 0 \\ \beta_2 & 0 & -\mu_2 \end{pmatrix}$$

and the linearized coupling dynamics is

$$\gamma = (d\mathbf{F})_{\mathbf{x}_{I_i,j}} = (d\mathbf{F})_{\mathbf{x}_{i,J_j}} = \begin{pmatrix} 0 & 0 & 0 \\ 0 & 0 & 0 \\ \beta_2 & 0 & 0 \end{pmatrix}.$$

As for the eigenvalues of the adjacency matrices, we established in Theorem 1 that N_1 and N_2 must be all-to-all connected networks for the antigenic variation model. An n-node all-to-all network adjacency matrix has the form

$$A_n = \begin{pmatrix} 0 & 1 & 1 & \dots & 1 \\ 1 & 0 & 1 & \dots & 1 \\ \vdots & & \ddots & & \vdots \\ 1 & \dots & & 0 & 1 \\ 1 & \dots & & 1 & 0 \end{pmatrix} \in \mathbb{R}^{n \times n}.$$

We now describe the eigenvalues of A_n in the following lemma.

Lemma 1. *The eigenvalues for the adjacency matrix of an n-node all-to-all coupled are $n-1$ and -1. The eigenvalues $n-1$ and -1 have multiplicities 1 and $n-1$, respectively.*

Proof. Since the row sum for each row in A_n is $n-1$, $n-1$ is going to be an eigenvalue with $(1, 1, \dots, 1)^T$ as its eigenvector. Furthermore, a direct calculation shows that -1 is also an eigenvalue and its associated $n-1$ eigenvectors are

$$\begin{pmatrix} -1 \\ 1 \\ 0 \\ 0 \\ \vdots \\ 0 \end{pmatrix}, \begin{pmatrix} -1 \\ 0 \\ 1 \\ 0 \\ \vdots \\ 0 \end{pmatrix}, \dots, \begin{pmatrix} -1 \\ 0 \\ 0 \\ 0 \\ \vdots \\ 1 \end{pmatrix}.$$

Therefore, the eigenvalue $n-1$ has multiplicity of 1 and the eigenvalue -1 has multiplicity of $n-1$. ∎

Since the linearized coupling for N_1 and N_2 are the same, we can simplify Eq. (4) to

$$M_{u,v} = \eta + (u+v)\gamma.$$

In general, each $M_{u,v}$ block has the form

$$M_{u,v} = \begin{pmatrix} \phi - \alpha_1 z - \alpha_2 w & -\alpha_1 y & -\alpha_2 y \\ \beta_1 & -\mu_1 & 0 \\ (1+u+v)\beta_2 & 0 & -\mu_2 \end{pmatrix}. \quad (5)$$

Given that $\mathrm{spec}(A_{n_1}) = \{n_1 - 1, -1\}$ and $\mathrm{spec}(A_{n_2}) = \{n_2 - 1, -1\}$, we only need to analyze the eigenvalues of M_{n_1-1,n_2-1}, $M_{n_1-1,-1}$, $M_{n_2-1,-1}$, and $M_{-1,-1}$ to know all the eigenvalues for J at each synchronous equilibrium. Instead of analyzing the eigenvalues of an $n_1 n_2 \times n_1 n_2$ matrix, we have reduced the analysis to only four 3×3 matrices at a synchronous equilibrium.

Theorem 3. *The trivial equilibrium $\mathbf{x}_1^*$ is always unstable.*

Proof. At $\mathbf{x}_1^*$, the general $M_{u,v}$ block for our system becomes

$$M_{u,v}(\mathbf{x}_1^*) = \begin{pmatrix} \phi & 0 & 0 \\ \beta_1 & -\mu_1 & 0 \\ (1+u+v)\beta_2 & 0 & -\mu_2 \end{pmatrix}.$$

Each $M_{u,v}$ block is lower triangular, so $\phi, -\mu_1$ and $-\mu_2$ are the roots of the corresponding characteristic polynomial regardless of the value of u and v. Given that these constants are positive for a biologically realistic model, there is always an unstable root ϕ. Hence, the system is always unstable at $\mathbf{x}_1^*$. ∎

4.2. *Local stability near* $\mathbf{x}_2^*$

We have shown in Theorem 3 that the trivial equilibrium $\mathbf{x}_1^*$ is always unstable. More importantly, we showed that the real part of any eigenvalues cannot be zero at this equilibrium for biologically realistic conditions (i.e. positive parameters). Hence, there would be no bifurcation from this equilibrium. In this section, we show in Theorem 4 that $\mathbf{x}_2^*$ can be asymptotically stable.

Theorem 4. *The nontrivial equilibrium $\mathbf{x}_2^*$ is locally asymptotically stable for appropriately small values of $\alpha_2 \beta_2$.*

Proof. At $\mathbf{x}_2^*$, the $M_{u,v}$ block becomes

$$M_{u,v}(\mathbf{x}_2^*) = \begin{pmatrix} 0 & -\alpha_1 y_2^* & -\alpha_2 y_2^* \\ \beta_1 & -\mu_1 & 0 \\ (1+u+v)\beta_2 & 0 & -\mu_2 \end{pmatrix},$$

and the corresponding characteristic polynomial is

$$\lambda^3 + a_1\lambda^2 + a_2\lambda + a_3 = 0,$$

where

$$a_1 = \mu_1 + \mu_2,$$

$$a_2 = \alpha_1\beta_1 y_2^* + \alpha_2\beta_2 y_2^*(1+u+v) + \mu_1\mu_2,$$

$$a_3 = \alpha_1\beta_1\mu_2 y_2^* + \alpha_2\beta_2\mu_1 y_2^*(1+u+v).$$

By the Routh–Hurwitz criterion, the equilibrium $\mathbf{x}_2^*$ is asymptotically stable at $\mathbf{x}_2^*$ if $a_1 > 0$, $a_3 > 0$, and $a_1 a_2 - a_3 > 0$. Through a direct calculation, the expression $a_1 a_2 - a_3$ is simplified to

$$a_1 a_2 - a_3 = (\alpha_1\beta_1\mu_1 + (1+u+v)\alpha_2\beta_2\mu_2)y_2^*$$

$$+ \mu_1\mu_2(\mu_1 + \mu_2).$$

Clearly, the expressions for a_1, a_3, and $a_1 a_2 - a_3$ are all positive for $u, v, |u+v+1| > 0$. We know from Lemma 1 that $u \in \text{spec}(A_{n_1}) = \{n-1, -1\}$ and $v \in \text{spec}(A_{n_2}) = \{m-1, -1\}$. For any nontrivial case of the system, M_{n_1-1,n_2-1}, $M_{u,-1}$, and $M_{-1,v}$ will always produce eigenvalues with negative real part.

Given that the eigenvalues from the other three blocks must all have negative real part, we focus on $M_{-1,-1}$. When $u, v = -1$, a_3 and $a_1 a_2 - a_3$ become

$$a_3 = (\alpha_1\beta_1\mu_2 - \alpha_2\beta_2\mu_1)y_2^*$$

and

$$a_1 a_2 - a_3 = (\alpha_1\beta_1\mu_1 - \alpha_2\beta_2\mu_2)y_2^*$$

$$+ \mu_1\mu_2(\mu_1 + \mu_2).$$

It is easy to see that for small enough combinations of $\alpha_2\beta_2\mu_2$, the stability condition from Routh–Hurwitz criterion is satisfied. Therefore, $\mathbf{x}_2^*$ can be locally asymptotically stable for small values of $\alpha_2\beta_2\mu_2$. ∎

4.3. *Bifurcation analysis*

To analyze the bifurcations from the synchronous nontrivial equilibrium $\mathbf{x}_2^*$, we introduce the concepts of balanced coloring and quotient network from [Golubitsky *et al.*, 2005] to aid the process.

The notion of balanced coloring is related to the inputs of each node and finding patterns of synchrony for the nodes in a coupled cell system. To start, we need to define the set of inputs for each node in the network.

Definition 4.1. For $c \in \mathcal{C}$, the *input set* of c is

$$I(c) = \{e \in \mathcal{E} : \mathcal{H}(e) = c\}.$$

An element of $I(c)$ is called an input edge or input arrow of c.

Definition 4.2. The relation $\sim_I$ of *input equivalence* on $\mathcal{C}$ is defined by $c \sim_I d$ if and only if there exists an arrow type preserving bijection

$$\beta : I(c) \to I(d).$$

That is, for every input arrow $i \in I(c)$

$$i \sim_\mathcal{E} \beta(i).$$

Any such bijection β is called an *input isomorphism* from node c to node d.

At a synchronous equilibrium, all the nodes have the same states. When subsets of nodes are synchronized with each other, these nodes may be equilibria, periodic or even chaotic states, forming a pattern of synchrony or a *polysynchronous subspace*. For a given polysynchronous subspace, we can define an equivalence relation $\bowtie$ such that the subspace is defined as

$$\Delta_\bowtie = \{\mathbf{x} \in P : c \bowtie d \Leftrightarrow \mathbf{x}_c = \mathbf{x}_d\},$$

where P denotes the appropriate phase space for $\mathbf{x}$. This equivalence relation partitions the nodes in synchrony into equivalence classes and it forms the polysynchronous subspace. We can define a specific type of equivalence relations based on the inputs received by each node [Golubitsky *et al.*, 2005]:

Definition 4.3. Suppose a coupled cell system is associated with digraph $\mathcal{G}$. Let the node set $\mathcal{C}$ denote the set of nodes of $\mathcal{G}$ and let $\mathcal{E}$ denote the set of edges of $\mathcal{G}$. An equivalence relation $\bowtie$ on the node set $\mathcal{C}$ is balanced if for every $c, d \in \mathcal{C}$ with $c \bowtie d$, there exists an input isomorphism β such that $\mathcal{T}(i) \bowtie \mathcal{T}(\beta(i))$ for $i \in \mathcal{I}(c)$, where $\mathcal{T}(i)$ is a function denoting the node at the end of edge i and $\mathcal{I}$ denotes the input set for c.

There can be many different equivalence relations for a given network. Based on a given balanced equivalence relation, one could associate a color for

each class of nodes. Hence, a balanced relation $\bowtie$ with k classes is equivalent to a balanced k-coloring of a digraph.

The notion of balanced equivalence is important in simplifying a coupled cell system. Based on a balanced equivalence relation $\bowtie$ on a network N, we can always reduce the system to a *quotient network* $N_\bowtie$. The dynamics of the reduced network can be *lifted* to the original network [Golubitsky *et al.*, 2005]. In other words, finding a balanced coloring allows one to analyze a reduced quotient system and any dynamics of the simpler system must also be in the original system. Suppose the network N has the node set $\mathcal{C} = \{c_1, \ldots, c_n\}$ and $\bowtie$ is a balanced equivalence relation on N with m classes. We outline the steps to construct the quotient network $N_\bowtie$ from N:

(1) Let $\bar{c}$ denote the $\bowtie$-equivalence class of $c \in \mathcal{C}$. The nodes in $\mathcal{C}_\bowtie$ are the $\bowtie$-equivalence classes in $\mathcal{C}$; that is,

$$\mathcal{C}_\bowtie = \{\bar{c} : c \in \mathcal{C}\}.$$

Thus we obtain $\mathcal{C}_\bowtie$ by forming the quotient of $\mathcal{C}$ by $\bowtie$, that is, $\mathcal{C}_\bowtie = \mathcal{C}/\bowtie$.

(2) Define

$$\bar{c} \sim_{\mathcal{C}_\bowtie} \bar{d} \Leftrightarrow c \sim_{C} d.$$

The relation $\sim_{\mathcal{C}_\bowtie}$ is well defined since $\bowtie$ refines $\sim_C$.

(3) Let $\mathcal{S} \subset \mathcal{C}$ be a set of nodes consisting of precisely one node c from each $\bowtie$-equivalence class. The input arrows for a quotient node $\bar{c}$ are identified with the input arrows in node c, where $c \in \mathcal{S}$, that is, $I(\bar{c}) = I(c)$.

When viewing the arrow $i \in I(c)$ as an arrow in $I(\bar{c})$, we denote that arrow by $\bar{i}$. Thus, the arrows in the quotient network are the projection of arrows in the original network formed by the disjoint union

$$\mathcal{E}_\bowtie = \dot{\bigcup_{c \in \mathcal{S}}} I(c).$$

The definition of the quotient network structure is independent of the choice of the representative nodes $c \in \mathcal{S}$.

(4) Two quotient arrows are equivalent when the original arrows are equivalent. That is,

$$\bar{i}_1 \sim_{\mathcal{E}_\bowtie} \bar{i}_2 \Leftrightarrow i_1 \sim_\mathcal{E} i_2,$$

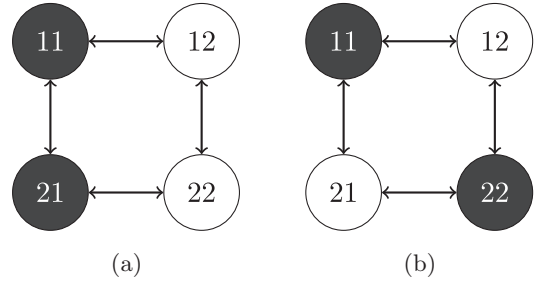where $i_1 \in I(c_1)$, $i_2 \in I(c_2)$, and $c_1, c_2 \in \mathcal{S}$.

(a) (b)

Fig. 2. Two different 2-coloring possible for the $S_2 \times S_2$ formulation of the system where each node represents system (2).

(5) Define the heads and tails of quotient arrows by

$$\mathcal{H}(\bar{i}) = \overline{\mathcal{H}(i)} \quad \text{and} \quad \mathcal{T}(\bar{i}) = \overline{\mathcal{T}(i)}.$$

(6) For $e_1, e_2 \in \mathcal{E}_\bowtie$, it is easy to verify that the quotient network satisfies that $e_1 \sim_{\mathcal{E}_\bowtie} e_2 \Rightarrow \mathcal{H}(e_1) \sim_{\mathcal{C}} \mathcal{H}(e_2)$ and $\mathcal{T}(e_1) \sim_{\mathcal{C}} \mathcal{T}(e_2)$. The quotient network is independent of the choice of nodes in $\mathcal{S}$ because $\bowtie$ is balanced.

In the above procedure, one node is chosen from each equivalence class in determining the arrow structure. Since all nodes in the same class of a balanced relation have isomorphic input sets, the choice of the nodes in each class of N does not matter. Mathematical details of constructing a quotient network from a coupled cell system can be found in [Golubitsky *et al.*, 2005].

For a given network, there can be many different k-colorings. For example, the network in Fig. 1 can have two different 2-coloring patterns and these patterns are illustrated in Fig. 2. In general, a network that has been reduced to its 2-coloring quotient network has the form in Fig. 3. Given that dynamics of the quotient network lifts to the original network, we will analyze the general 2-color quotient network with each node representing system (2). We will show that synchrony-breaking Hopf bifurcation occurs in the antigenic variation model. Each node of network in Fig. 3 represents
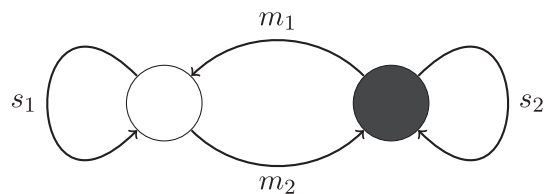

Fig. 3. Minimizing the number of arrows used in Fig. 2 with s_i representing the number of self-connections and m_i the number of external connections.

$$\frac{dy_i}{dt} = y_i(\phi - \alpha_1 z_i - \alpha_2 w_i),$$

$$\frac{dz_i}{dt} = \beta_1 y_i - \mu_1 z_i, \tag{6}$$

$$\frac{dw_i}{dt} = \beta_2((s_i + 1)y_i + m_i y_j) - \mu_2 w_i,$$

where i denotes the index for one node and j denotes the index for the other node in Fig. 3.

$$h = \frac{\alpha_1 \beta_1 \mu_2 + \alpha_2 \beta_2 \mu_1 (s_1 + s_2 - n_c + 1)}{\alpha_1^2 \beta_1^2 \mu_2^2 + \alpha_1 \beta_1 \mu_2 \alpha_2 \beta_2 \mu_1 (s_1 + s_2 + 2) + \alpha_2^2 \beta_2^2 \mu_1^2 ((s_1 + 1)(s_2 + 1) - m_1 m_2)}$$

and

$$k = \frac{\alpha_1 \beta_1 \mu_2 n_c + \alpha_2 \beta_2 \mu_1 ((s_1 + 1)(s_2 + 1) - m_1 m_2)}{\alpha_1^2 \beta_1^2 \mu_2^2 + \alpha_1 \beta_1 \mu_2 \alpha_2 \beta_2 \mu_1 (s_1 + s_2 + 2) + \alpha_2^2 \beta_2^2 \mu_1^2 ((s_1 + 1)(s_2 + 1) - m_1 m_2)},$$

are constants by the parameters of the system. These terms are results of the configuration of the 2-color quotient network.

The nontrivial equilibrium is always positive for the system formed according to Theorem 1 because of its configuration, but this property does not hold for all 2-color quotient networks for the system. With certain combination of the parameters, the nontrivial equilibrium for the reduced system can have negative components due to the terms $(s_1 + s_2 - n_c + 2)$ and $((s_1 + 1)(s_2 + 1) - m_1 m_2)$ in the expressions for h and k. Different configuration of systems formed using system (2) resulting in possible negative values for the nontrivial equilibrium is consistent with the results in [De Leenheer & Pilyugin, 2008a]. To keep our analysis biologically realistic, we assume that the combination of parameters and the number of arrows for the system produce a positive nontrivial equilibrium. In other words, we now assume that the choice of parameters and configuration always give positive h and k.

Based on the aforementioned assumption, we will analyze possible bifurcations for system (6). Conditions for Hopf bifurcation are stated in the following theorem.

Theorem 5. *For system* (6), *2-color synchrony-preserving bifurcations cannot occur from* $\mathbf{x}_2^{\bowtie}$. *If*

$$\frac{\alpha_1 \beta_1 \mu_2}{\alpha_2 \beta_2 \mu_1} > n_c - (1 + s_1 + s_2) > \frac{\alpha_1 \beta_1 \mu_1}{\alpha_2 \beta_2 \mu_2}, \tag{7}$$

then synchrony-breaking Hopf bifurcation occurs from $\mathbf{x}_2^{\bowtie}$ *when*

Suppose $\mathbf{x}_i^{\bowtie}$ represents the equilibrium expression for each node of the quotient network. The point $\mathbf{x}_1^{\bowtie} = (0,0,0)^T$ is the synchronous trivial equilibrium and the synchronous nontrivial equilibrium point $\mathbf{x}_2^{\bowtie}$ is given by

$$\mathbf{x}_2^{\bowtie} = \begin{pmatrix} y_2^{\bowtie} \\ z_2^{\bowtie} \\ w_2^{\bowtie} \end{pmatrix} = \begin{pmatrix} \phi \mu_1 \mu_2 h \\ \phi \beta_1 \mu_2 h \\ \phi \beta_2 \mu_1 k \end{pmatrix},$$

where

$$\phi = \frac{\mu_1 + \mu_2}{h(\alpha_2 \beta_2 \mu_2 (n_c - (1 + s_1 + s_2)) - \alpha_1 \beta_1 \mu_1)}.$$

Proof. The Jacobian for the 2-color quotient system is

$$J = \begin{pmatrix} \eta + s_1 \gamma & m_1 \gamma \\ m_2 \gamma & \eta + s_2 \gamma \end{pmatrix},$$

where $\eta(\mathbf{x}_i^{\bowtie}, \phi)$ is the matrix of linearized internal dynamics and $\gamma(\mathbf{x}_i^{\bowtie}, \phi)$ is the matrix of the linearized coupling dynamics. This Jacobian matrix has the same structure as the case studied in [Golubitsky *et al.*, 2005]. We see that $n_c = s_1 + m_1 = s_2 + m_2$. Let $\mathbf{v} \in \mathbb{R}^3$, then

$$J \begin{pmatrix} \mathbf{v} \\ \mathbf{v} \end{pmatrix} = \begin{pmatrix} (\eta + n_c \gamma)\mathbf{v} \\ (\eta + n_c \gamma)\mathbf{v} \end{pmatrix}$$

and

$$J \begin{pmatrix} m_1 \mathbf{v} \\ -m_2 \mathbf{v} \end{pmatrix} = \begin{pmatrix} (\eta + (s_1 + s_2 - n_c)\gamma)m_1 \mathbf{v} \\ -(\eta + (s_1 + s_2 - n_c)\gamma)m_2 \mathbf{v} \end{pmatrix}.$$

Hence, the combined eigenvalues of $\eta + n_c \gamma$ and $\eta + (s_1 + s_2 - n_c)\gamma$ are the eigenvalues of J.

Given that $n_c, s_1 + s_2 - n_c \in \mathbb{Z}$, we shall study the eigenvalues for the general matrix $\eta + n\gamma$ for any $n \in \mathbb{Z}$. The corresponding characteristic polynomial for $\eta + n\gamma$ block is

$$\lambda^3 + a_1 \lambda^2 + a_2 \lambda + a_3 = 0,$$

where

$$a_1 = \mu_1 + \mu_2,$$

$$a_2 = \phi\mu_1\mu_2 h(\alpha_1\beta_1 + \alpha_2\beta_2(1 + n)) + \mu_1\mu_2,$$

$$a_3 = \phi\mu_1\mu_2 h(\alpha_1\beta_1\mu_2 + \alpha_2\beta_2\mu_1(1 + n)).$$

By the Routh–Hurwitz criterion, the $\mathbf{x}_2^{\bowtie}$ is asymptotically stable if $a_1 > 0$, $a_3 > 0$, and $a_1 a_2 - a_3 > 0$. Through a direct calculation, the expression $a_1 a_2 - a_3$ simplifies to

$$a_1 a_2 - a_3 = \phi\mu_1\mu_2 h(\alpha_1\beta_1\mu_1 + (1 + n)\alpha_2\beta_2\mu_2)$$

$$+ \mu_1\mu_2(\mu_1 + \mu_2). \qquad (8)$$

Clearly, the expressions for a_1, a_3, and $a_1 a_2 - a_3$ are all positive for $n > 0$. For any formulation of the system, all the eigenvalues of the block $\eta + n_c\gamma$ always have negative real part. Given that $(\mathbf{v}, \mathbf{v})^T \in \Delta = \{(\mathbf{x}, \mathbf{x})^T \in (\mathbb{R}^3)^2\}$ is the eigenvector associated with the $\eta + n_c\gamma$ block, we will not have any synchrony preserving bifurcation from $\mathbf{x}_2^{\bowtie}$.

We now focus our attention on the $\eta + (s_1 + s_2 - n_c)\gamma$ block to find possible Hopf bifurcation. A Hopf bifurcation occurs if the conditions $a_1 > 0$ and $a_3 > 0$ hold true while $a_1 a_2 - a_3$ crosses from the positive to the negative as a parameter of the system varies [Yu, 2005]. For all parameter values, a_1 is always positive and a_3 is positive by the assumption in the first inequality of (7). Hence, the Hurwitz conditions for local stability are satisfied.

For the bifurcation analysis, we choose ϕ as the bifurcation parameter. We see that for small enough ϕ, $a_1 a_2 - a_3$ is necessarily positive. For bifurcation to occur, the expression

$$\phi\mu_1\mu_2 h(\alpha_1\beta_1\mu_1 + (1 + s_1 + s_2 - n_c)\alpha_2\beta_2\mu_2)$$

$$+ \mu_1\mu_2(\mu_1 + \mu_2)$$

must cross from positive to negative. Given that all the parameters of the system are positive, the previous expression can only be negative if

$$\frac{\alpha_1\beta_1\mu_1}{\alpha_2\beta_2\mu_2} < n_c - (1 + s_1 + s_2).$$

Hence, we require the second inequality of Eq. (7). As ϕ increases, the system reaches the critical point when $a_1 a_2 - a_3 = 0$. Given that ϕ is linear in $a_1 a_2 - a_3$, we can isolate ϕ in $a_1 a_2 - a_3 = 0$ to obtain the bifurcation condition. Because the eigenvector associated with $\eta + (s_1 + s_2 - n_c)\gamma$ is $(m_1\mathbf{v}, -m_2\mathbf{v})^T$ and it is obviously not part of the synchrony subspace. Therefore, there can only be synchrony-breaking bifurcation from $\mathbf{x}_2^{\bowtie}$. $\blacksquare$

For the 2-coloring shown in Fig. 2(a), $n_c = 2$, $s_i = 1$ and $m_i = 1$. A direct calculation shows that $2 - (1 + 1 + 1) = -1$. Since all the parameters are positive constants, the necessary condition in (7) cannot be satisfied and this pattern does not occur via Hopf bifurcation. On the other hand, the 2-coloring shown in Fig. 2(b), $n_c = 2$, $s_i = 0$ and $m_i = 2$ and the necessary condition can be satisfied based on the selection of parameters. The synchrony-breaking Hopf bifurcation from $\mathbf{x}_2^{\bowtie}$ to this pattern will be considered numerically in the next section.

5. Numerical Simulations

In this section, we use numerical tools to demonstrate the analytic results obtained in earlier sections. For any system formed by Theorem 1, we have shown in Theorem 5 that there exists a 2-color pattern associated with a synchrony-breaking Hopf bifurcation from the nontrivial synchronous equilibrium. To show these analytical results, we fix the parameters at $\alpha_1 = 10^{-3}$, $\alpha_2 = 10^{-3}$, $\beta_1 = 10^{-4}$, $\beta_2 = 10^{-4}$, $\mu_1 = 1/100$ and $\mu_2 = 1/50$ [Blyuss & Gupta, 2009] and use ϕ as the bifurcation parameter as shown in Theorem 5.

5.1. System with four strains

In Fig. 4, we see that for $\phi = 0.5$ the system in Fig. 2 is at the nontrivial equilibrium. As we increase the bifurcation value to $\phi = 1.5$, we see that oscillations from synchrony-breaking bifurcation occur as shown in Fig. 5. Clearly, nodes 11 and 22 are synchronized and nodes 12 and 21 are also synchronized. Based on this configuration, the inequality in (7) is satisfied with our selection of parameters. We also see that these two sets of nodes are out of phase by $T/2$, where T is the period of the periodic solution. These results agree with the synchrony-breaking subspace being supported by $(m_1\mathbf{v}, -m_2\mathbf{v})^T$. Given that $m_1 = m_2 = 2$ in this case, the amplitudes of the oscillations for the nodes are also in agreement with the earlier theoretical results.

5.2. System with eight strains

To show that the method presented in this paper works for larger systems, we form a system with
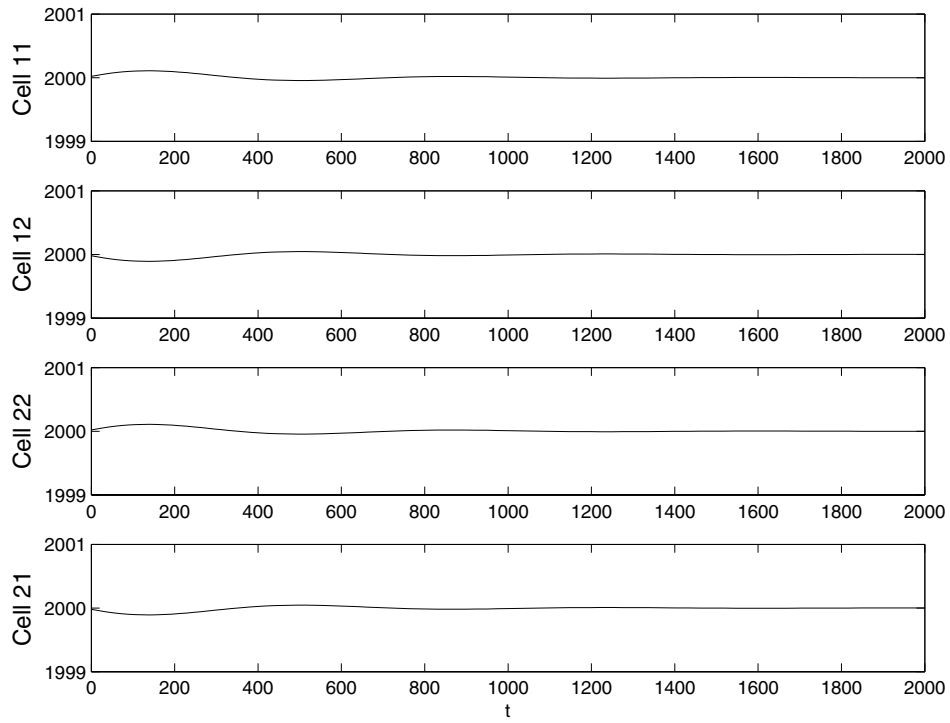
Fig. 4.   Simulated pathogen populations (y_{ij}) of the system shown in Fig. 1 for $\phi = 0.5$: A nontrivial synchronous equilibrium.
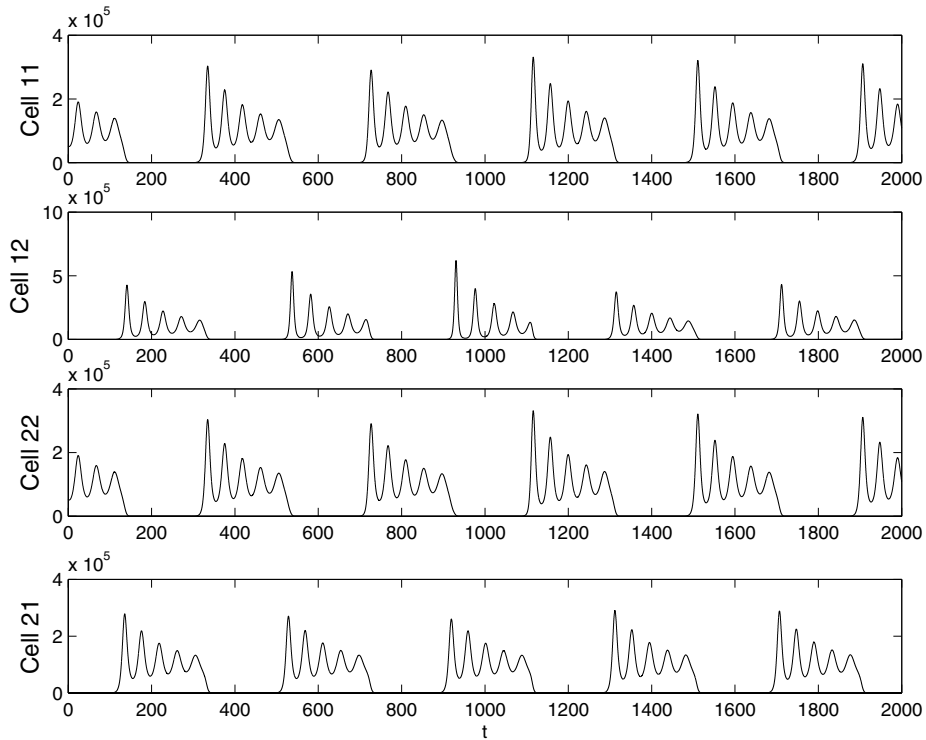

Fig. 5.   Simulated pathogen populations (y_{ij}) of the system shown in Fig. 1 for $\phi = 1.5$: Hopf bifurcation.
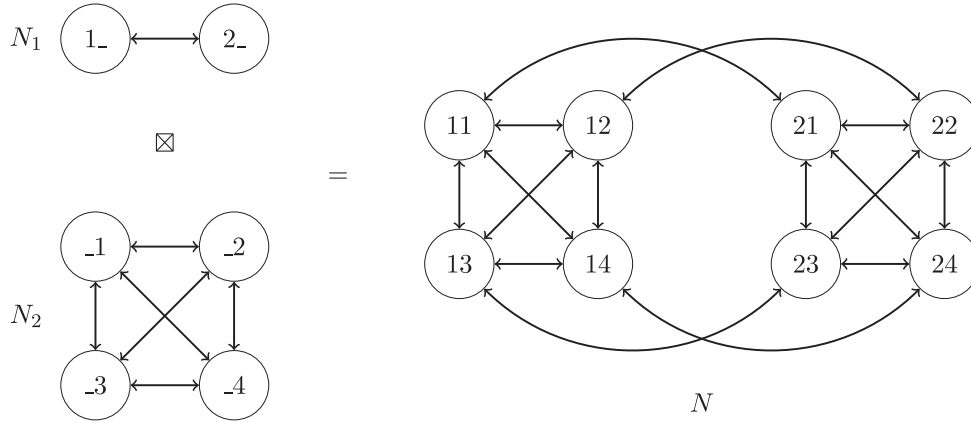
Fig. 6. A network modeling the eight strains formed by two networks with $n_1 = 2$ and $n_2 = 4$.

$n_1 = 2$ and $n_2 = 4$. This configuration is depicted in Fig. 6. Numerical simulations of this configuration are shown in Figs. 7 and 8. The solutions shown in these figures are in periodic synchrony that is in accordance to the configurations in Figs. 9(a)

and 9(b), respectively. The two different color patterns in Fig. 9 are produced using different initial conditions.

The two patterns in Fig. 9 both have the quotient parameters $s_1 = s_2 = 1$. Hence, the number
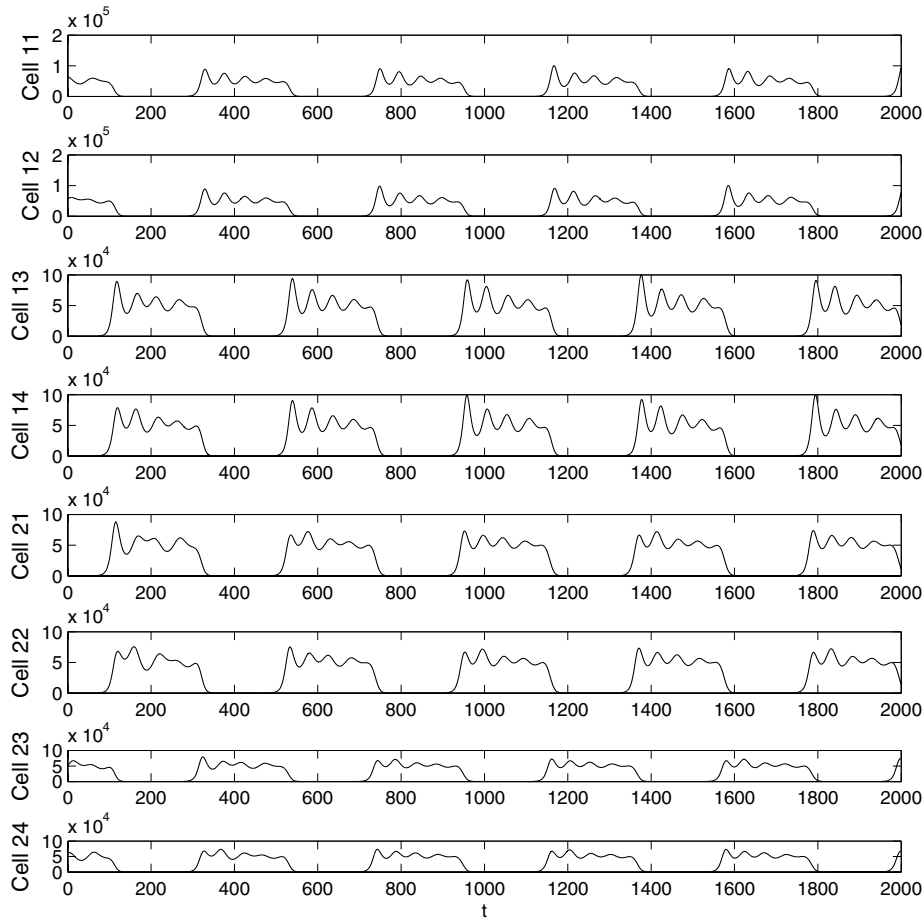

Fig. 7. Simulated pathogen populations (y_{ij}) of the system shown in Fig. 6 for $\phi = 1$: 2-color pattern, in agreement with Fig. 9(a).
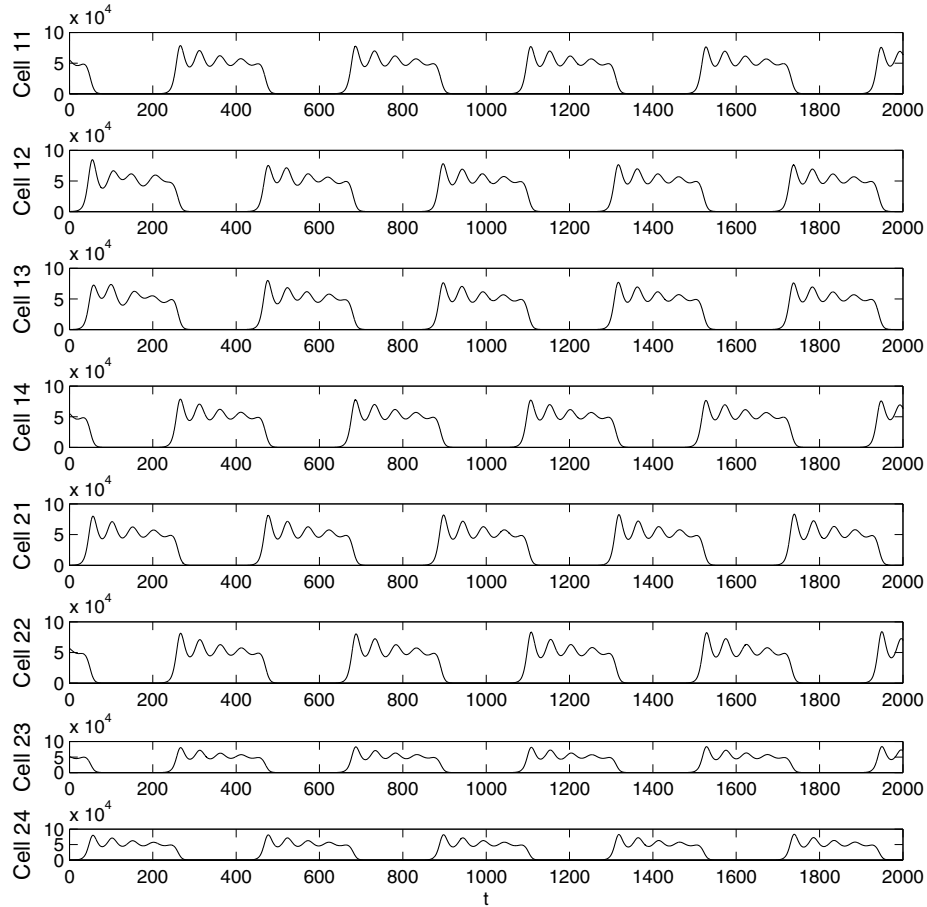
Fig. 8. Simulated pathogen populations (y_{ij}) of the system shown in Fig. 6 for $\phi = 1$: 2-color pattern, in agreement with Fig. 9(b).
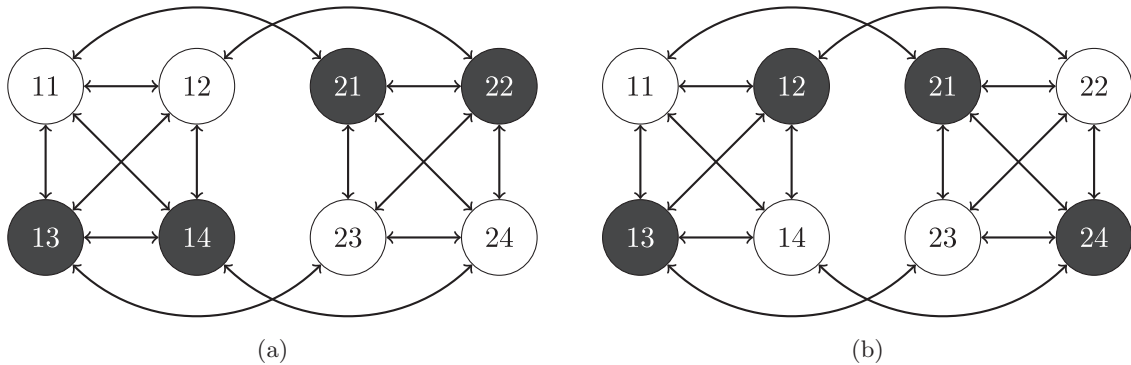

Fig. 9. These are two synchrony patterns consistent with the results found analytically in Theorem 5 and numerical results in Figs. 7 and 8. These patterns correspond to $s_1 = s_2 = 1$ and $m_1 = m_2 = 3$ for the 2-color quotient network.

of white nodes coupled to a white node is the same number of black nodes coupled to a black node for all the aforementioned patterns. In the numerical simulations of these cases [Figs. 9(a) and 9(b)], the solutions for the two classes are out of phase by half the period. The phase shifted solutions here agree with the results for the 4-strain system as well as the work by Golubitsky *et al.* [2005, Corollary 9.3].

6. Conclusions and Discussions

In our mathematical analysis, we have shown in Theorem 1 that the general system described in

[Blyuss & Gupta, 2009] can be formulated using the product network method discussed in [Golubitsky & Lauterbach, 2009]. The digraphs used in this paper to represent the networks are different from those used by Blyuss and Gupta [2009], but they represent the same system because these systems are equivalent in the sense of [Dias & Stewart, 2005]. The formulation of the model as two all-to-all networks allows us to analyze the linear stability at any fully synchronous equilibrium. Instead of directly dealing with an $n_1 n_2 \times n_1 n_2$ matrix, we have reduced the analysis to four 3×3 matrices. Analytically, it is difficult to determine the eigenvalues for large matrices. Our reduction allows one to directly analyze the stability at the trivial equilibrium. As stated in Theorem 3, the trivial synchronous equilibrium is always unstable. This result is important because we have shown that any possible dynamics from a fully synchronous equilibrium must arise from the nontrivial equilibrium.

We have also obtained the necessary condition in (7) for the nontrivial equilibrium to be stable and that for Hopf bifurcation to occur in Theorem 5. In the proof, we have shown that any type of synchrony-preserving dynamics cannot arise form the nontrivial synchronous equilibrium through bifurcation. Mathematically, we have ruled out the possible dynamics. By ruling out synchrony-preserving bifurcation in this model, we have shown that the bifurcation dynamics is consistent with this biological behavior for antigenic variation. As stated in [Craig & Scherf, 2003], it is important that variants are not expressed at the same time for antigenic variation to be a successful strategy for the pathogen. Our results imply that any synchrony pattern arising from bifurcation would be consistent with this biological requirement for antigenic variation.

Other than ruling out synchrony-preserving bifurcation, Theorem 5 also shows that synchrony-breaking Hopf bifurcation can arise from this nontrivial equilibrium. In [Recker *et al.*, 2004], the authors showed numerically that in some parameter ranges oscillations occur for the model (3) and these oscillations described hierarchies of the sequential appearance of variants. In this paper, we have showed that the numerical pattern which corresponds to the hierarchy of sequential immunodominant is a result of bifurcations and it corresponds to 2-color patterns of synchrony.

Furthermore, for antigenic variation to be a successful immune escape strategy, it is essential that the pathogen must have the ability for some variants to be expressed while others stay relatively dormant [Craig & Scherf, 2003]. It must also be able to switch from the actively expressed variants to the dormant variants. Analytically, we have shown that the increase in growth rate will eventually cause the system to go from the nontrivial synchronous equilibrium to a synchrony-breaking Hopf bifurcation and the switching mechanism is the Hopf bifurcation. The peaks and valleys in the oscillations may correspond to the active and dormant requirement of antigenic variation.

The condition in Eq. (7) shows that not all variants can necessarily be synchronized and synchronization patterns must be based on the same condition. This condition is based on the parameters of the system and the number of self-connections in the 2-color quotient system. We can rule out some patterns directly. For example, the pattern shown in Fig. 2(a) corresponds to $s_1 = s_2 = 1$ and $m_1 = m_2 = 1$ in the 2-color quotient network. We can see that the inequality in (7) cannot be satisfied for any biologically meaningful parameter values.

As shown by Blyuss and Gupta [2009], the strain space investigated in this work has $S_{n_1} \times S_{n_2}$ symmetry. Other authors of intra-host multistrain models, such as Dawes and Gog [2002], Gog and Swinton [2002], have also purposed strain spaces that have symmetry in them. This symmetry in the strain space is based on the assumption that all combination of epitopes are viable. However, only certain combinations of the epitopes on the pathogens may work for their target cells [Craig & Scherf, 2003]. Thus, the strain space for a given pathogen may not necessarily be symmetric. The general coupled cell method used here does not require any specific symmetry, so our approach might be more suitable to investigate further specific biological scenarios.

Biologically, these 2-color patterns correspond to all variants being synchronized in two separate groupings. These separate groups are out of phase by half of the period of the oscillations. The 2-color synchrony-breaking Hopf bifurcation fits the requirement for antigenic variation to occur when expressing variants and at different time as well as other synchronized variants that stay relatively dormant over time oscillations. Given that multiple

variants are expressed at the same time in a 2-color pattern, it reduces the potential effectiveness of immune escape. The limitation of two groupings barely fits the minimum of two variants needed for features of antigenic variation as outlined in [Turner, 2002]. The framework set out by Golubitsky *et al.* [2005] can be used to analyze k-coloring and therefore it is possible to study finite number of variants in synchrony-breaking patterns in future works.

For future work, we can expand the analysis in this paper by specifically analyzing patterns that may be more biologically relevant. As the number of the major variants in the model gets higher, there are many more patterns, making it impossible to enumerate all these patterns. One can certainly take advantage of the framework of k-colorings provided in [Golubitsky *et al.*, 2005]. We believe that the extension of our work from 2-color bifurcations to k-color bifurcation would provide a more realistic analysis for the model.

One can also further the research by modifying assumptions made in this paper. In simplifying the calculations, we have assumed that all strains have identical parameters. Our analysis can be extended to incorporate different parameters for different strains by altering the coupled cell representation. Instead of having only one type of nodes in the digraph, different shapes of nodes can be used to denote strains with different parameters.

Aside from the identical parameters assumption, we have also restricted the analysis to only 2-colorings of the systems. Again, we made this assumption to simplify the calculations. Since each color in a coloring pattern corresponds to one cluster, our analysis can only produce patterns with two different groups of synchrony. A more general analysis for larger number of colors in the colorings can generate more possible patterns.

Acknowledgments

References

Blyuss, K. & Gupta, S. [2009] "Stability and bifurcations in a model of antigenic variation in malaria," *J. Math. Biol.* **58**, 923–937.

Craig, A. & Scherf, A. [2003] *Antigenic Variation* (Academic Press).

Dawes, J. & Gog, J. [2002] "The onset of oscillatory dynamics in models of multiple disease strains," *J. Math. Biol.* **45**, 471–510.

De Leenheer, P. & Pilyugin, S. [2008a] "Immune response to a malaria infection: Properties of a mathematical model," *J. Biol. Dyn.* **2**, 102–120.

De Leenheer, P. & Pilyugin, S. [2008b] "Multistrain virus dynamics with mutations: A global analysis," *Math. Med. Biol.* **25**, 285.

Dias, A. & Stewart, I. [2005] "Linear equivalence and ODE-equivalence for coupled cell networks," *Nonlinearity* **18**, 1003.

Frank, S. & Barbour, A. [2006] "Within-host dynamics of antigenic variation," *Infect. Gen. Evol.* **6**, 141–146.

Gog, J. & Swinton, J. [2002] "A status-based approach to multiple strain dynamics," *J. Math. Biol.* **44**, 169–184.

Golubitsky, M., Stewart, I. & Török, A. [2005] "Patterns of synchrony in coupled cell networks with multiple arrows," *SIAM J. Appl. Dyn. Syst.* **4**, 78–100.

Golubitsky, M. & Stewart, I. [2006] "Nonlinear dynamics of networks: The groupoid formalism," *Bull. Amer. Math. Soc.* **43**, 305.

Golubitsky, M. & Lauterbach, R. [2009] "Bifurcations from synchrony in homogeneous networks: Linear theory," *SIAM J. Appl. Dyn. Syst.* **8**, 40.

Gravenor, M. & Lloyd, A. [1998] "Reply to: Models for the in-host dynamics of malaria revisited: Errors in some basic models lead to large over-estimates of growth rates," *Parasitology* **117**, 409–410.

Mitchell, J. & Carr, T. [2010] "Oscillations in an intra-host model of *Plasmodium falciparum* malaria due to cross-reactive immune response," *Bull. Math. Biol.* **72**, 590–610.

Mitchell, J. & Carr, T. [2012] "Synchronous versus asynchronous oscillations for antigenically varying *Plasmodium falciparum* with host immune response," *J. Biol. Dyn.* **6**, 333–357.

Recker, M., Nee, S., Bull, P., Kinyanjui, S., Marsh, K., Newbold, C. & Gupta, S. [2004] "Transient cross-reactive immune responses can orchestrate antigenic variation in malaria," *Nature* **429**, 555–558.

Saul, A. [1998] "Models for the in-host dynamics of malaria revisited: Errors in some basic models lead to large over-estimates of growth rates," *Parasitology* **117**, 405–407.

Turner, C. [2002] "A perspective on clonal phenotypic (antigenic) variation in protozoan parasites," *Parasitology* **125**, 17–24.

Yu, P. [2005] "Closed-form conditions of bifurcation points for general differential equations," *Int. J. Bifurcation and Chaos* **15**, 1467–1483.